Analysis of consistency between B- and G-stations records for induced events in the Groningen gas field.

Final Report

Document N° : STR_FUG_18P17_01

SEISTER

SEISMIC ENGINEERING SOLUTIONS

Date : 08/07/2019

Prepared for : FUGRO

FUGRO

Analysis of consistency between B- and G-stations records for induced events in the Groningen gas field.

Document N°: STR_FUG_18P17_01

Client

Fugro NL Land B.V.

Veurse Achterweg 10, 2264 SG Leidschendam | Postbus 9440, 9703 LP Groningen, Nederland

Email

@fugro.com

Supplier

SEISTER SAS
Immeuble Cap Sud
106 Avenue Marx Dormoy
92120 Montrouge
France

Email

@seister.fr

Contract N°

1018-0338-999

Revision n° : 0

Number of pages : 31

	Authors	Verification	Approval
Date	08/07/2019	08/07/2019	08/07/2019
Name			

Version	Date	Status	Description
0	19/04/2019	draft	Initial version
1	29/04/2019	final	Final version after consideration of comments from reviewers
2	08/07/2019	final	Includes an Addendum (Annex 2) with two additional figures upon request of SodM

Table of contents

1. Introduction and objectives

Within the framework of the KEM04 project "Data driven study on seismic structural features of Groningen ground motions", an important task is the collection and analysis of the recorded ground motions for the induced events in the field. The induced earthquakes are recorded at the KNMI stations consisting of two networks: the B and G networks. These data are publicly accessible from the KNMI website and have been downloaded by the project team. The B network consists of accelerometers at the surface (EpiSensor starting from 2014) whereas the G stations consists of a vertical array of 1 accelerometer (EpiSensor) at the surface (called G0) and 4 geophones at 50m, 100m, 150m and 200m depth. Only records at the surface are considered in this Report.

Records from these networks are used in the project to:

1. Investigate the features of the Groningen ground motion records (spatial variability, vertical motion, attenuation);
2. Calibrate and validate the 3D simulations of wave propagation performed using the SPEED code;
3. Test the GMM V5 in order to assess its performance in reproducing the observed ground motion records.

The reliability of recorded motions at these stations is thus of paramount importance for the project.

A consistency analysis between recordings at closely located B and G0 stations was presented in the MEMO N° 18P17_05022019 in February 2019 (hereafter referred to as MEMO) based on data downloaded from the KNMI portal on late November 2018. One of the conclusions of the MEMO was that there was a systematic difference between ground motion recorded at B and G0 stations that was probably related to instrumentation issues.

After the MEMO and the following discussions, KNMI communicated that an error was found in the parameterization of the G0 sensors that caused recordings of such sensors being about a factor of 2 smaller than what they should be. The G0 data were corrected by KNMI *on December 17, 2018* and they are available from their portal.

The objective of this document is to repeat some of the analyses performed in the MEMO using the corrected G0 data in order to evaluate the effect of the correction. Some additional analyses are also performed (e.g., considering acceleration response spectra) upon request from The Dutch State Supervision of Mines (SodM). All the analyses are performed using Matlab® and related functions.

2. Records processing

The raw data were downloaded from the KNMI portal (http://rdsa.knmi.nl/dataportal) on March 2019 (after that the correction to the G0 stations was applied by KNMI). We considered the following set of data:

- Magnitude $M_L \geq 2$ (29 events after 09/2013);
- Stations located within 5 km buffer from Groningen gas field
- Horizontal and vertical components
- Surface and borehole records (only surface records are discussed in this document)

The records are processed based on PEER/RESORCE (Akkar et al., 2014) processing scheme (Figure 2-1).

The processing includes a filtering step. The identification of the low- and high-cut frequencies is based on the analysis of the signal-to-noise ratio (SNR). First, noise, P-wave and S-wave windows are identified based on manual picking of P- and S- arrival times and on the scheme defined in Kishida et al. (2014) and modified for the Groningen region (Figure 2-2 left). In particular the end time of the S-

wave window was automatically selected using an assumed S-wave duration and is expressed as follows:

$$Ds = Td_{rup} + Td_{prop}$$

where Td_{rup} is related to the rupture (source) duration and Td_{prop} is the duration through the propagation of the S-wave to the site and to scattering along the path. According to Kishida et al. (2014) Td_{rup} is found to be larger than the theoretical source duration. We considered Td_{rup} = 2s and Td_{prop} =0.18 Rh , where Rh is the hypocentral distance. The 0.18 coefficient for Td_{prop} is slightly larger than the one proposed by Kishida et al. (2014) but it was found appropriate for the Groningen recordings based on visual inspection of selected windows.

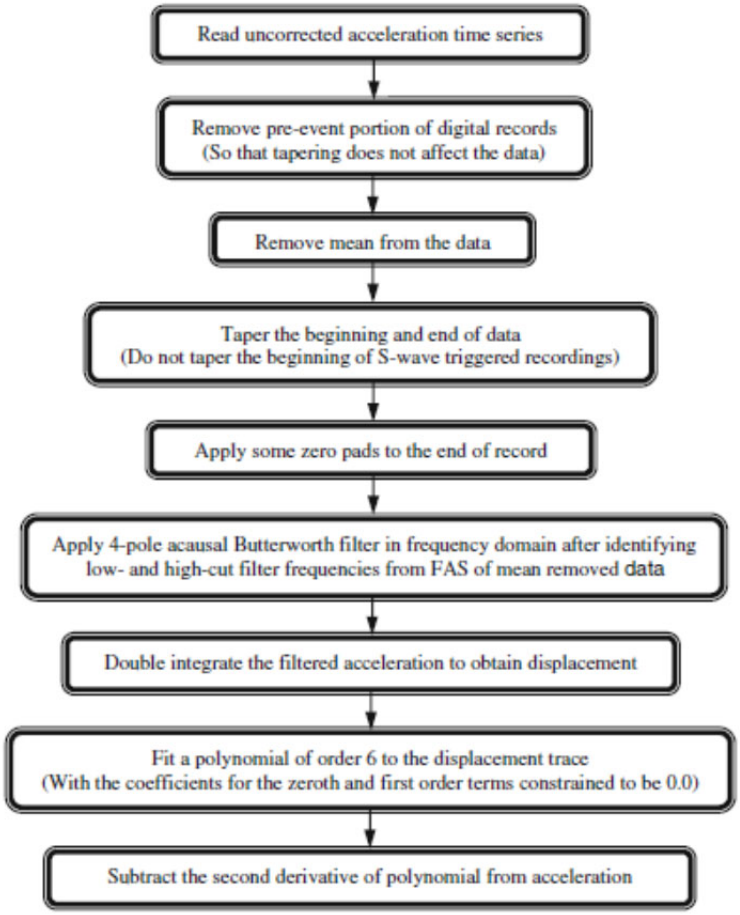

Figure 2-1 : Flow-chart of the processing used for the Groningen records also used in the RESORCE and PEER strong-motion database (from Akkar et al., 2014).

Fourier spectra are computed for the noise window as well as for the S-wave window, and for the total record duration defined as the S-waves arrival time + 25 s (Figure 2-2 middle). SNR are computed from the S-wave and the noise windows, and the frequency band with an SNR≥3 is identified (Figure 2-2 right). The full waveform is then filtered between the low- and high-cut frequencies identified. Note that a minimum threshold of 0.2 Hz is imposed to the low-cut frequency of the filter in order to avoid low-frequency trends not removed by the previously detailed procedure. The following exclusion criteria are applied to the records (meaning that the records are discarded and not used in subsequent analyses):

- maximum $f_{low\text{-}cut}$ for the 3 components is higher than 5.0 Hz;
- minimum $f_{high\text{-}cut}$ for the 3 components is lower than 5.0 Hz;
- minimum bandwidth $f_{low\text{-}cut}$ - $f_{high\text{-}cut}$ for the 3 components is lower than 5.0 Hz .

Examples of the results of this step of the processing are shown in Figure 2-2 and Figure 2-3 for two stations with different level of noise.

In order to optimize the procedure, the manual picking of P- and S-waves is done for the Zeerijp recordings only and, based on such results, simple functions for estimating the arrival times are developed and used for the other events (Figure 2-4). Because the relatively small extension of the gas field, the close source-to-site distances and the relatively homogenous velocity structure, we believe that such approximation is appropriate for this study. In any case, a visual screening is performed for each record based on plots as in Figure 2-2 in order to assess the appropriateness of the windows.

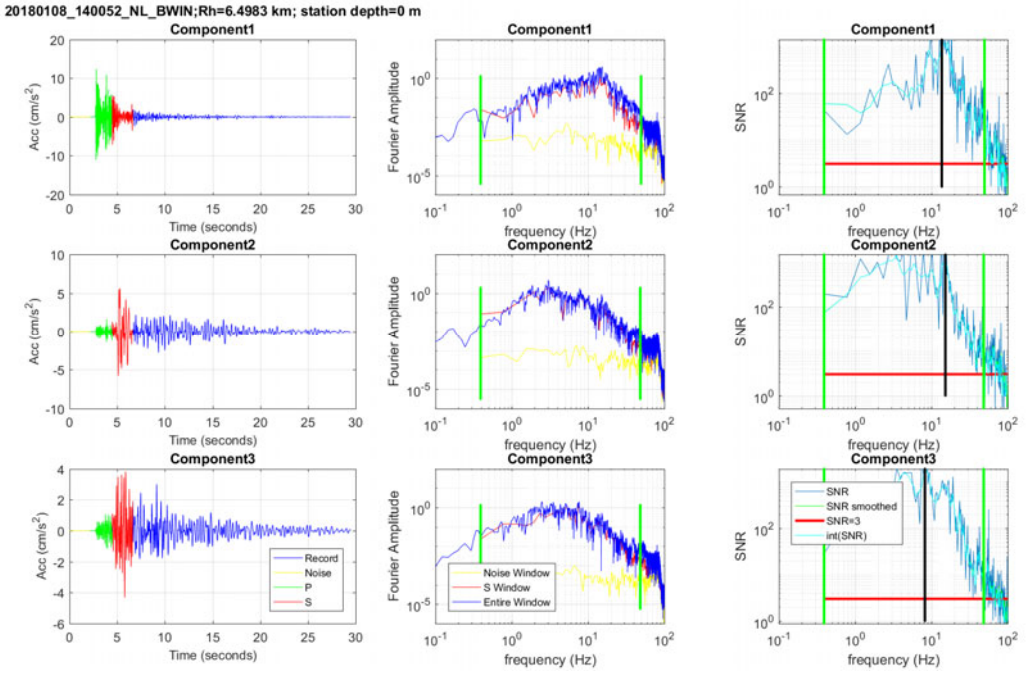

Figure 2-2 : Event 20180108_140052, station BWIN. Example of identification of P-waves, S-waves and noise windows, calculation of signal to noise (SNR) ratios and identification of high-cut and low-cut frequencies of the filter. The black line (right graphs) represents the frequency corresponding to the largest SNR.

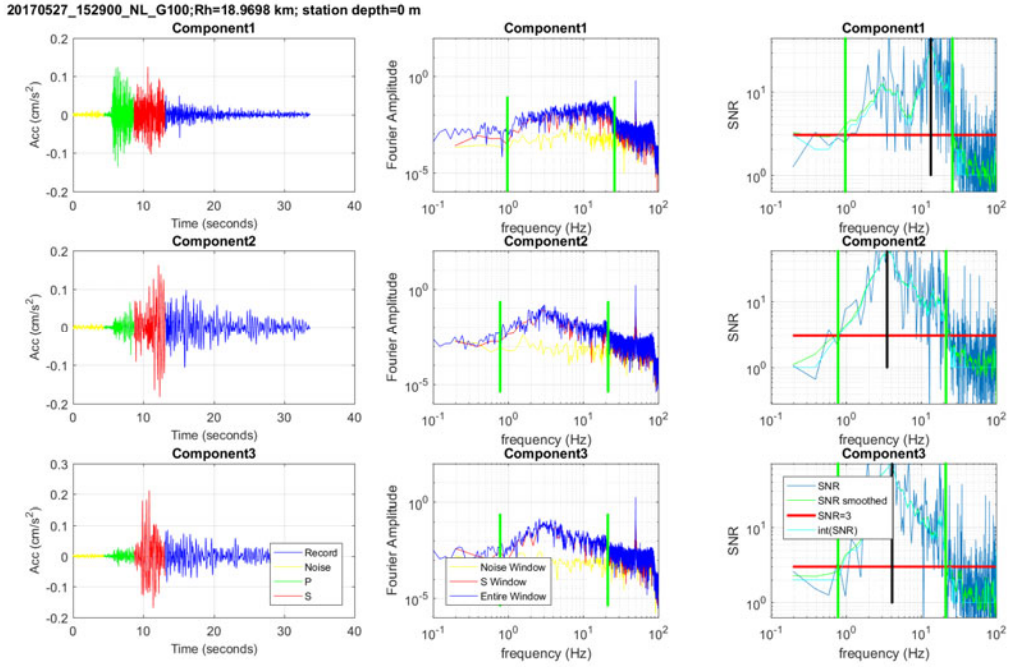

Figure 2-3 : Event 20170527_152900, station G100. Example of automatic identification of P-waves, S-waves and noise windows, calculation of signal to noise (SNR) ratios and identification of high-cut and low-cut frequencies of the filter. The black line (right graphs) represents the frequency corresponding to the largest SNR.

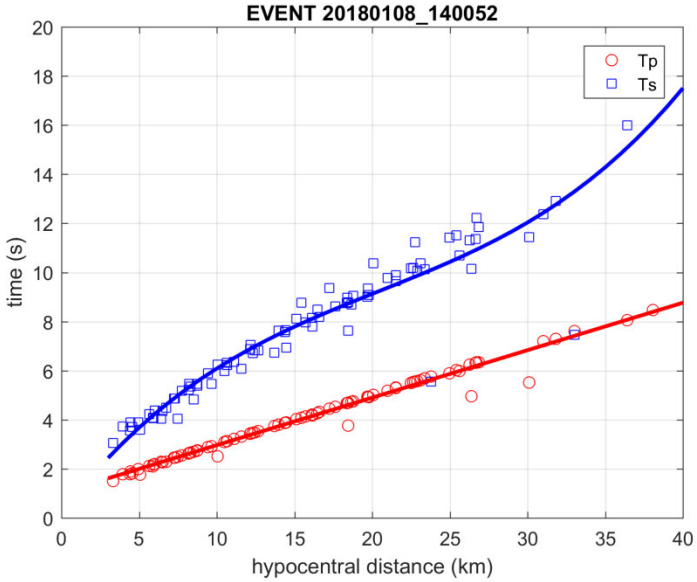

Figure 2-4 : Arrival times of P-waves (red circles) and S-waves (blue squares) based on manual picking of recordings for the Zeerijp event. The curves show the derived polynomial functions used to infer P and S arrival times for the other events.

3. Comparison of recordings at B and G stations

Several B and G stations are located very close to each other, having an inter-station distance of few hundred meters up to about 1.5 km. As a consistency analysis, similarly to what done in the MEMO, we selected pairs of B and G stations located close to each other and compared the records from the recorded events (Figure 3-1). On average, we expected to observe similar ground motions because of the similar wave propagation from the source to the two stations and relatively homogenous local site conditions.

The comparison is performed in terms of B-to-G spectral ratios from the records of each event, both in terms of acceleration Fourier amplitude spectra (FAS) and acceleration response spectra (PSA).

Table 3-1 reports the considered B-G station pairs, their inter-station distance and the number of records available for each pair (after the record processing).

We note that for some pair (i.e., BHKS-G290 and BZN1-G140) only one or two records are available and thus the results are not significant and are only presented for completeness. Other B stations (e.g., BONL, BGAR, BWSE, BWIR) are relatively far from a G station and the calculation of spectral ratios is not meaningful for the purpose of checking the consistency among B and G stations. In this case, other techniques (e.g., generalized inversion approaches, Ameri et al., 2011) may be applied to highlight the differences between B and G stations taking into account the relative source-to-site distance and considering a common reference site condition.

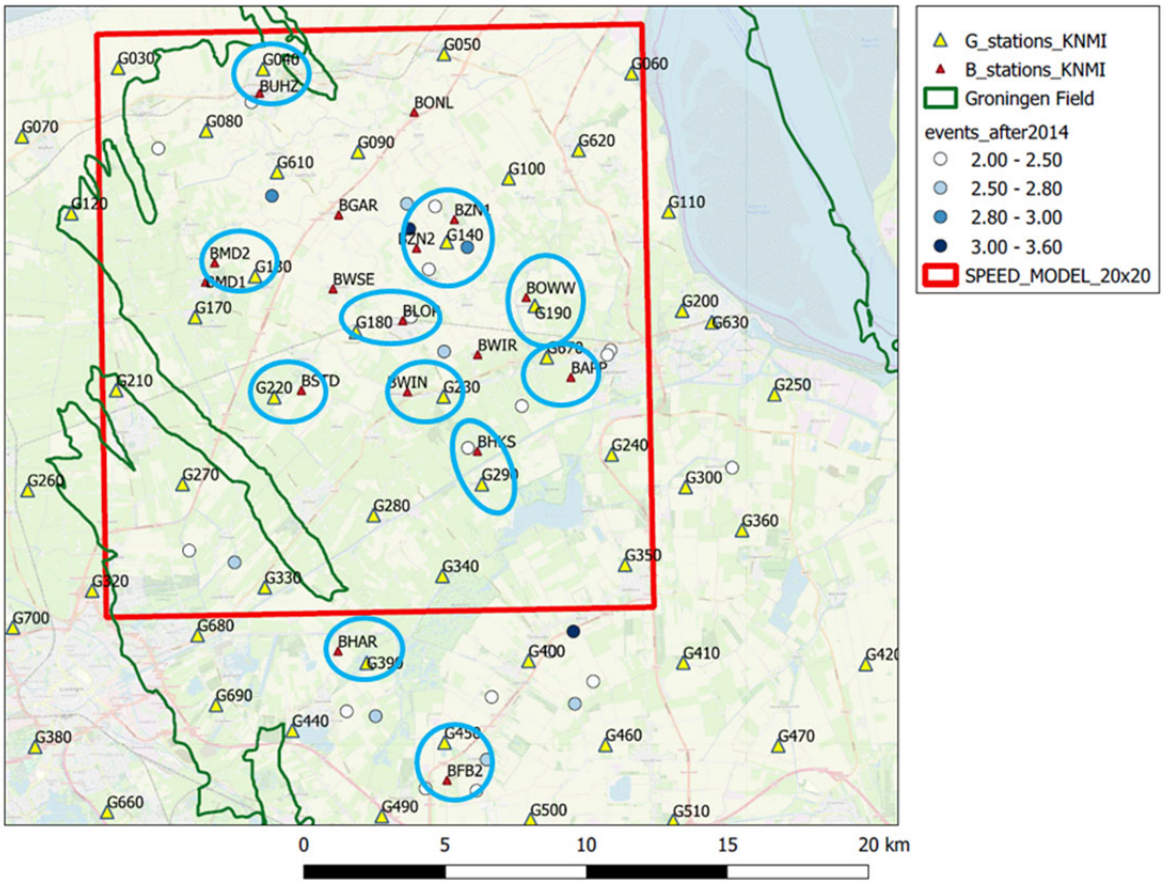

Figure 3-1 : Selected pairs of B and G0 stations in the Groningen field.

Table 3-1: B-G stations pairs considered in the analyses. Relative inter-station distance and number of available records are reported.

B-G pair	Inter-station distance (km)	N. of available records (FAS)	N. of available records (PSA)
BOWW-G190	0.43	9	8
BWIN-G230	1.29	8	7
BSTD-G220	0.99	13	10
BUHZ-G040	0.86	5	2
BZN2-G140	1.09	5	5
BMD2-G130	1.50	6	3
BHAR-G390	1.10	10	8
BAPP-G670	1.11	8	7
BFB2-G450	1.34	14	10
BLOP-G180	1.70	10	8
BHKS-G290	1.18	1	1
BZN1-G140	0.84	2	2

3.1 B-to-G ratios of acceleration Fourier amplitude spectra (FAS)

This section presents the comparisons in terms of acceleration Fourier amplitude spectra (FAS), similarly to what done in the MEMO (here we consider all available recorded events). Ratios between FAS recorded at adjacent B and G stations are calculated for the each event providing recordings at both stations. This is done for the horizontal (geometric mean of as-recorded horizontal components) and vertical components. As described in section 2, the records are processed and filtered and only Fourier spectra within the usable frequency band are considered for calculating the spectral ratios. FAS are smoothed using the Konno-Ohmachi (1998) algorithm with the b-parameter set equal to 40.

Figure 3-2 and Figure 3-3 show B to G stations FAS ratios for the considered pairs, for the horizontal and vertical components, respectively.

For the horizontal component, we observe that for some pairs (i.e., BOWW-G190, BZN2-G140) the mean ratios oscillate around 1 over the considered frequency range, as expected. However, for several other pairs (e.g., BWIN-G230, BHAR-G390, BSTD-G220) the ratios are around 1 in the low-frequency range (up to about 3Hz) and then they decrease to values significantly smaller than 1 towards higher frequencies. In other words, the accelerations recorded at several B stations are significantly smaller than those at the adjacent G stations in the high-frequency range.

Looking at FAS ratios for each recorded events (gray curves in Figure 3-2) we note that there is a general consistency of the spectral ratios and despite some variability, the FAS ratios for each event confirm the observations above. Some variations can be observed for certain pairs and are likely related to the fact that one station could be closer to one or more events event than the other station. This is the case for example of BLOP-G190 where the spectral ratios larger than 1 in the low-frequency range are related to the events in the Zeerijp region closer to BLOP station (see Figure 3-1).

For the vertical components (Figure 3-3) the FAS ratios are on average around 1 for most of the station pairs, although some deviation is visible particularly in the high-frequency range for some pair (e.g., BZN2-G140, BWIN-G230, BAPP-G670). These deviations are, on average, at higher frequencies with respect to what observed for the horizontal component.

Figure 3-4 and Figure 3-5 show the ratios for all events and all pairs of stations for the horizontal and vertical components, respectively. These figures further illustrate that, on average, over all the considered stations pairs, there is a systematic decrease of the horizontal B-to-G FAS ratios towards high frequencies with the average ratio being about 1 up to 3 Hz and decreasing to about 0.5 at 30 Hz. This effect is not visible on the vertical component where the B-to-G FAS ratios are on average around 1 over the considered frequency range.

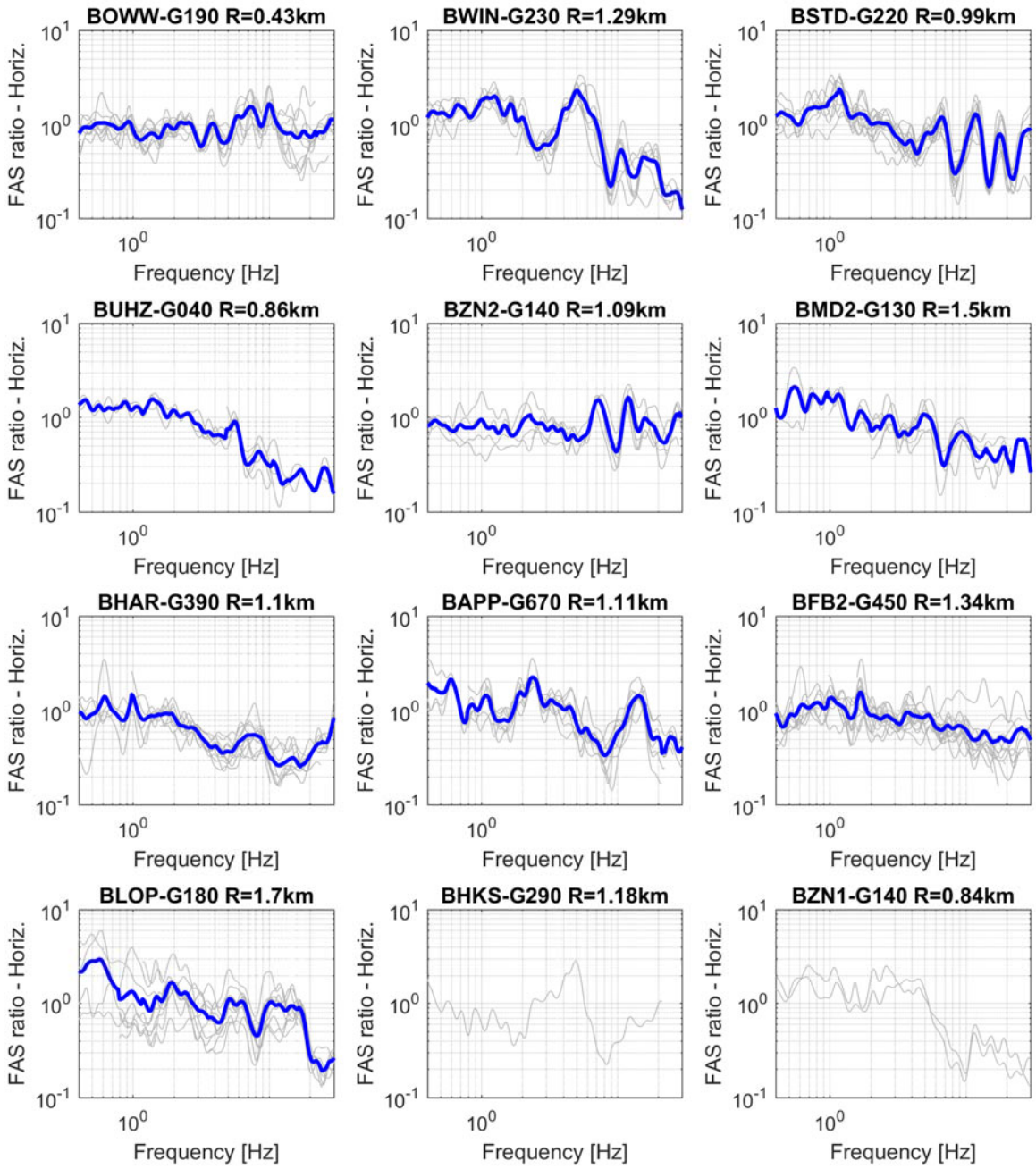

Figure 3-2 : Horizontal B-to-G Fourier Amplitude Spectra (FAS) ratio plotted for each pair of stations and for each recorded event (in gray). The geometric mean of horizontal components is considered. Mean ratios (only for pairs with at least 3 recordings) are shown in blue. The inter-station distance is shown in the graphs. Only FAS within the usable frequency band are plotted and considered for calculating the mean spectral ratios.

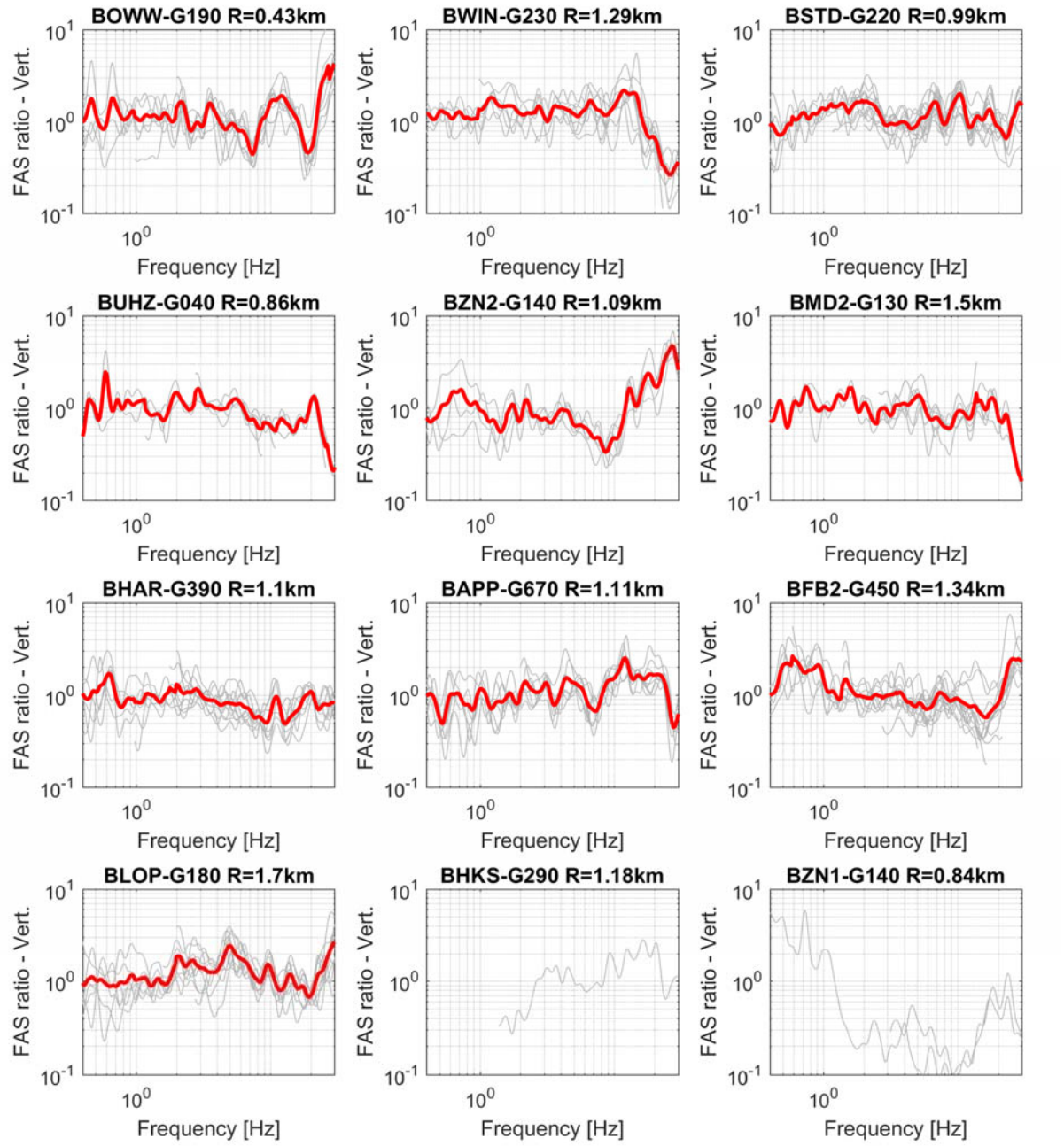

Figure 3-3 : Vertical B-to-G Fourier Amplitude Spectra (FAS) ratio plotted for each pair of stations and for each recorded event (in gray). Mean ratios (only for pairs with at least 3 recordings) are shown in red. The inter-station distance is shown in the graphs. Only FAS within the usable frequency band are plotted and considered for calculating the mean spectral ratios.

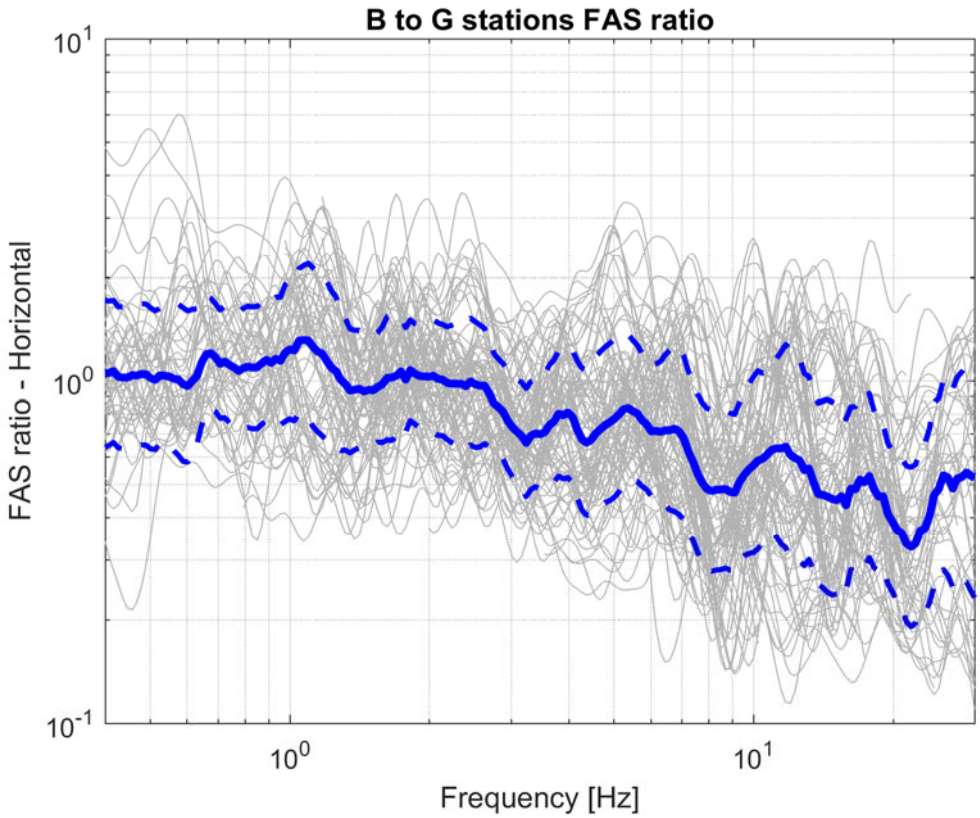

Figure 3-4 : Horizontal B-to-G Fourier Amplitude Spectra (FAS) ratio plotted for all considered pairs of stations and all events. The median ratio and its standard deviation are shown in blue.

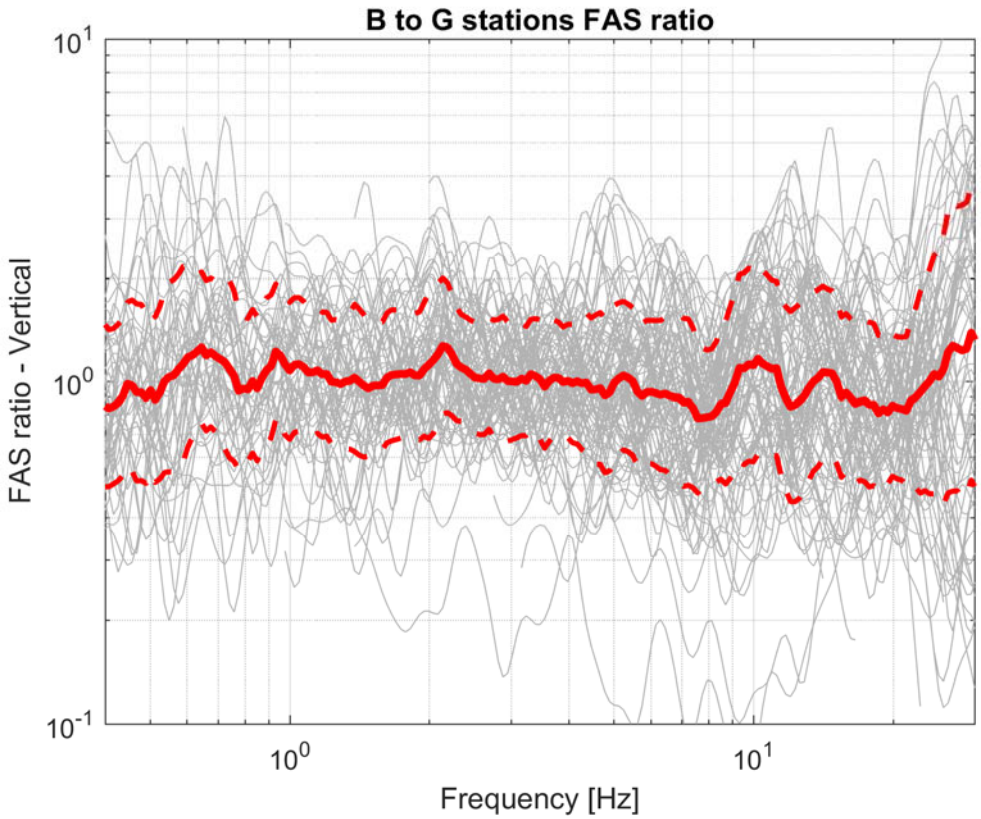

Figure 3-5 : Vertical B-to-G Fourier Amplitude Spectra (FAS) ratio plotted for all considered pairs of stations and all events. The median ratio and its standard deviation are shown in red.

3.2 B-to-G ratios of acceleration response spectra (PSA)

The comparison presented in the previous section are repeated here in terms of pseudo-spectral acceleration (PSA), at 5% damping, which is the measure used in the GMM V5 (and previous versions) for the hazard and risk calculations. This is done upon request of SodM.

Also in this case, the spectral ratios are computed considering the usable frequency band that we defined based on the filter cut-off frequencies during the processing phase of the records (section 2). However, because response spectra are sensitive to the filtering also in proximity to the applied cut-off frequencies, different usable frequencies are identified with respect to the FAS case. In particular, the minimum usable frequency is defined as 1.1*f_lowcut (the frequency of the low-cut filter), also consistent with recommendations of Akkar and Bommer (2006) and to what done in the GMM V4-V5 development. The maximum usable spectral frequency is defined as 100 Hz but only records with f_highcut >= 20 Hz (the frequency of the high-cut filter) are used for the calculation of the PSA ratios in order to have a reliable comparison of PGA (F=100 Hz).

Figure 3-6 and Figure 3-7 show B to G stations PSA ratios for the considered pairs, for the horizontal (geometric mean of as-recorded horizontal components) and vertical components, respectively.

Figure 3-8 and Figure 3-9 show the PSA ratios for all events and all pairs of stations for the horizontal and vertical components, respectively.

The comments made above considering the FAS ratio apply also to the PSA ratios although the shape of the spectral ratio is of course different. Moreover, due the necessary limit imposed to the f_highcut, a smaller number of records is available for certain pairs when considering response spectra compared to FAS consequently reducing the robustness of the results for PSA.

Figure 3-8 depicts, similarly to the FAS case, the systematic decrease of the horizontal B-to-G PSA ratios towards high frequencies with the average ratio being about 1 up to about 2 Hz and decreasing to about 0.6 at 100 Hz. This effectively means that recorded PGA at the considered B stations is on average 40% lower than that recorded at the considered G stations.

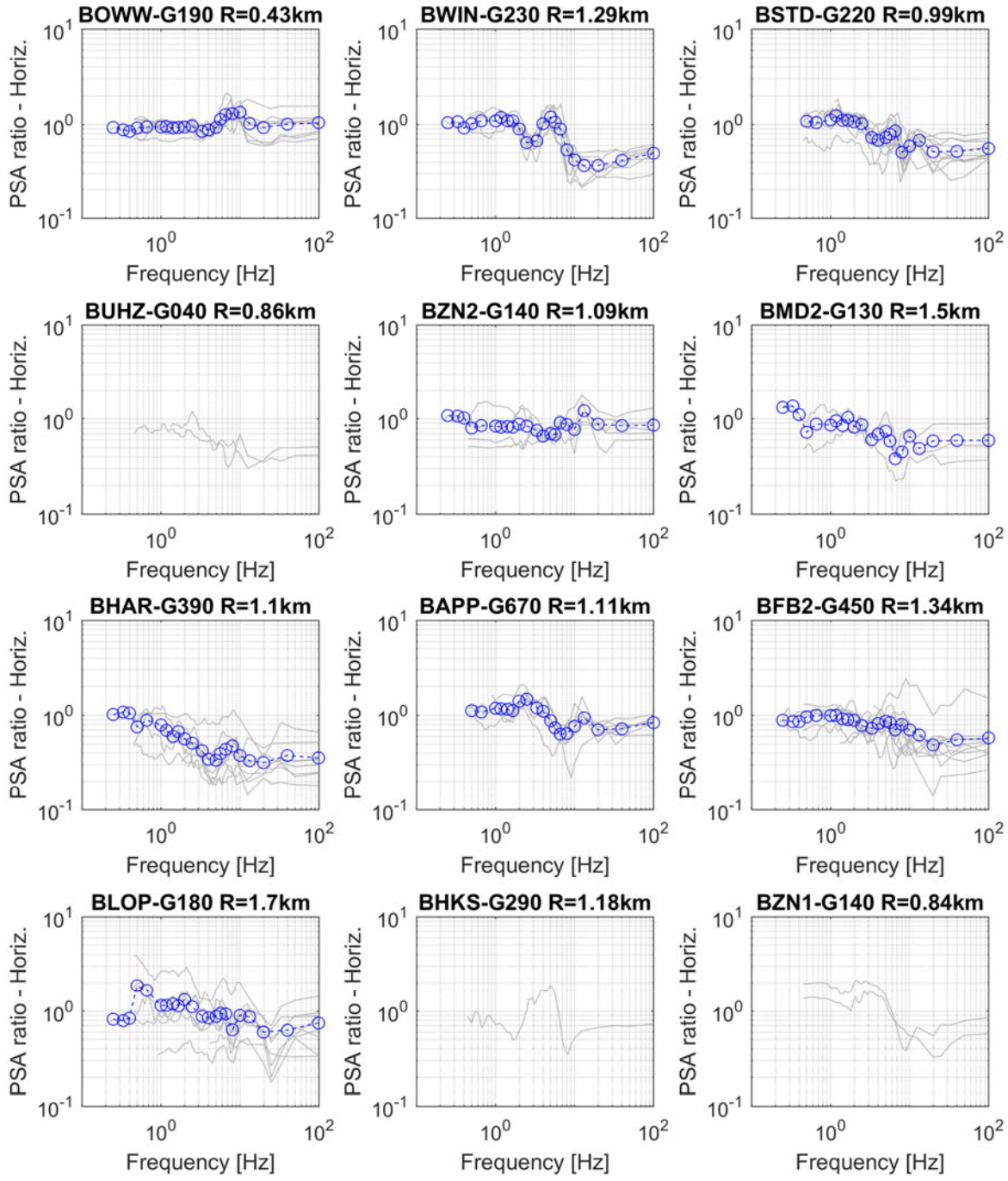

Figure 3-6 : Horizontal B-to-G spectral acceleration (PSA) ratio plotted for each pair of stations and for each recorded event (in gray). The geometric mean of horizontal components is considered. Mean ratios (only for pairs with at least 3 recordings) for the 23 spectral frequencies of the GMM V5 are shown in blue. The inter-station distance is shown in the graphs. Only PSA within the usable frequency band are plotted and considered for calculating the mean spectral ratios.

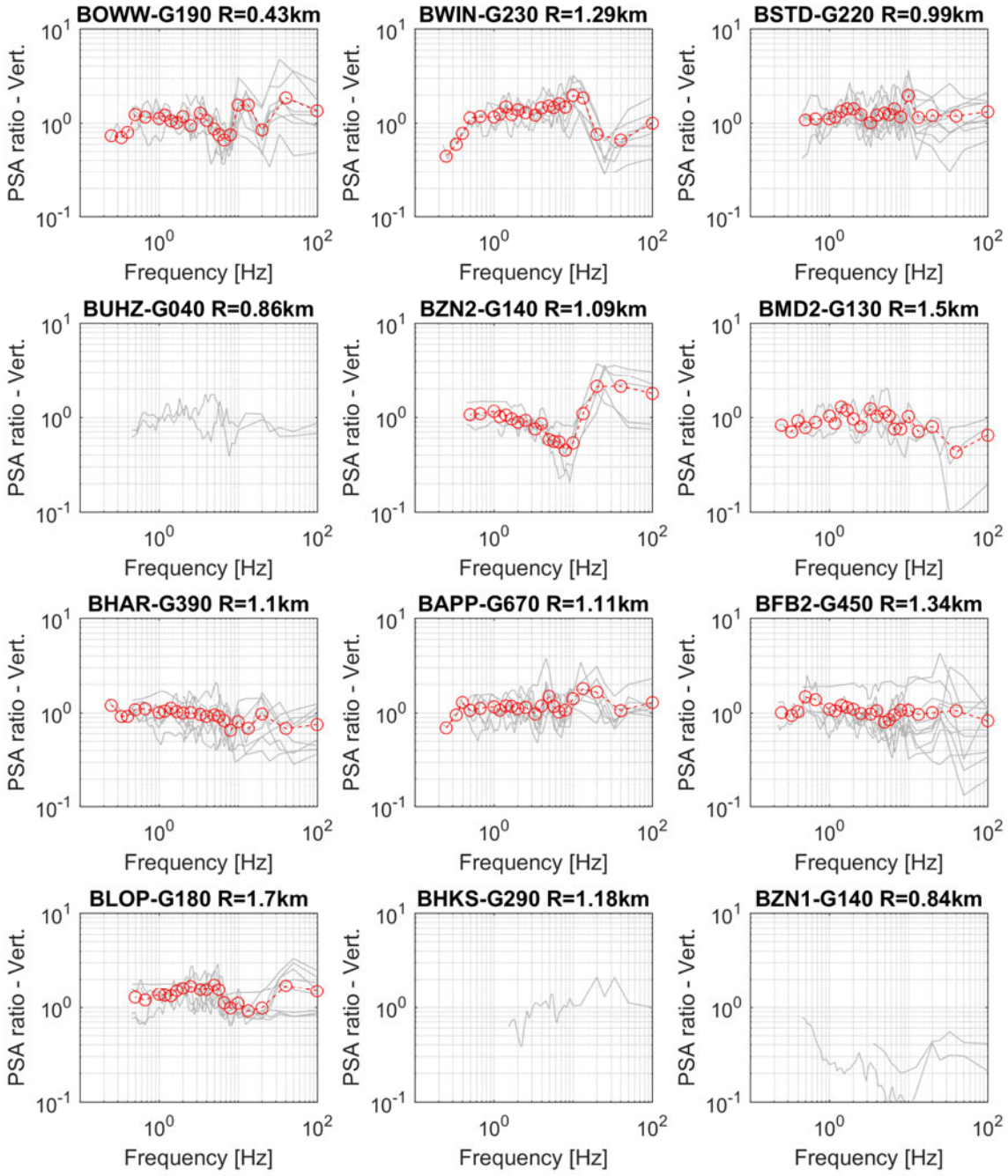

Figure 3-7 : Vertical B-to-G spectral acceleration (PSA) ratios plotted for each pair of stations and for each recorded event (in gray). The vertical component is considered. Mean ratios (only for pairs with at least 3 recordings) for the 23 spectral frequencies of the GMM V5 are shown in red. The inter-station distance is shown in the graphs.

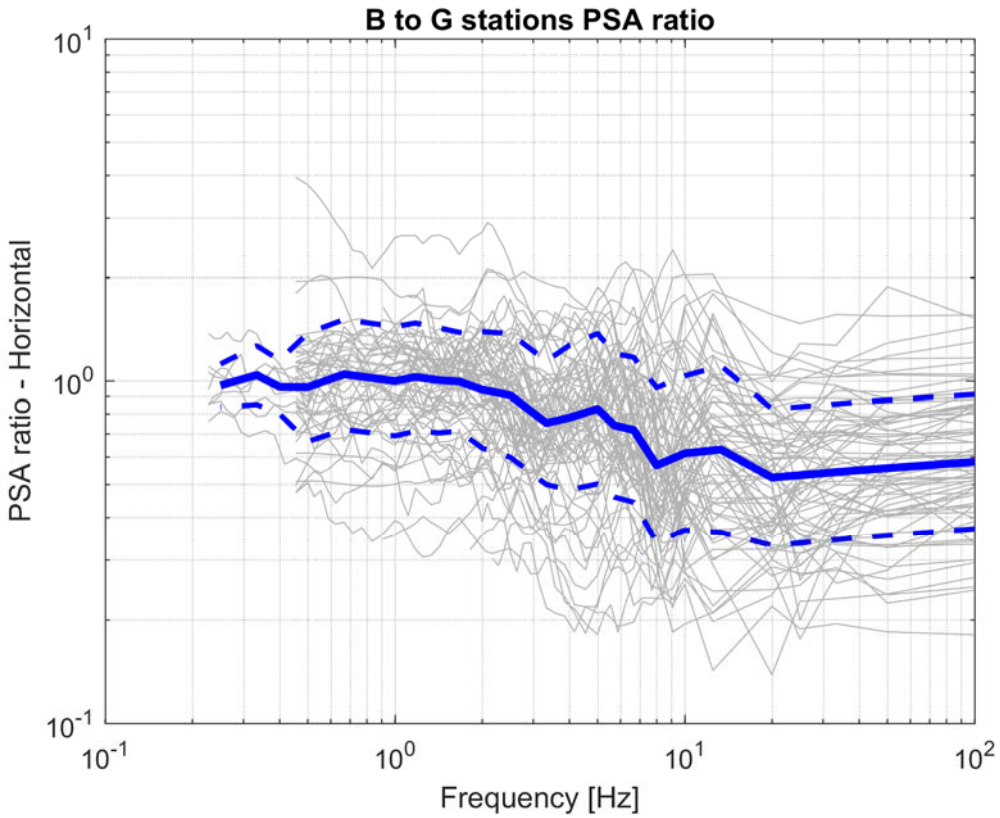

Figure 3-8 : Horizontal B-to-G spectral acceleration (PSA) ratios plotted for all considered pairs of stations and all events. The median ratio and its standard deviation are shown in blue.

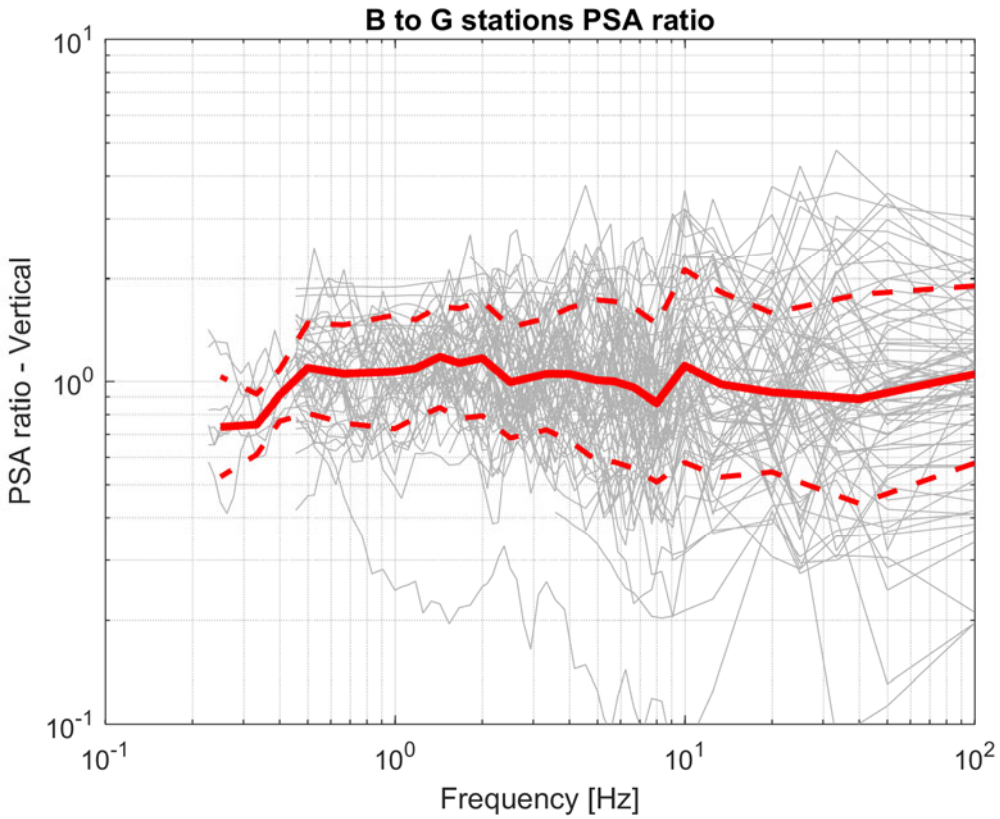

Figure 3-9 : Vertical B-to-G spectral acceleration (PSA) ratios plotted for all considered pairs of stations and all events. The median ratio and its standard deviation are shown in red.

4. Comparison of recordings among G stations

In order to better understand the origin of the unexpected amplitude differences between records at B and G stations at high frequencies, we performed the same comparison for pairs of G stations. In this case, the inter-station distance is larger and we can expect larger variations of the spectral ratios. However, if a sufficiently large number of pairs and records are considered we would expect, also in this case, to observe spectral ratios on average around 1. The selected pairs of G0 stations are shown in Figure 4-1 and their interstation distance and number of records are reported in Table 4-1.

As we can see, the pairs of G0 stations have much larger inter-station distance compared to the B-G pairs and the spectral ratios are not always meaningful when analyzed at single pairs (because large or small ratios may be just due to the local soil differences or to one station being much closer to the epicenter). For this reason only figures showing the spectral ratios for all events and all pairs together are shown in this report. Moreover, the purpose here is not to investigate specific G stations but simply to check whether we observe the same overall effect when considering all G stations pairs and all recorded events.

Figure 4-2 and Figure 4-3 show the G-to-G stations FAS ratios for all events and all pairs of stations for the horizontal and vertical components, respectively. The same is shown in Figure 4-4 and Figure 4-5 in terms of PSA.

Despite the larger inter-station distance between pairs of G stations, we do not observe any systematic effect and the median ratios are around 1 (slightly larger at high frequencies for the horizontal component probably related to local differences in the uppermost soil layers). We also note that, compared to the B-to-G ratios, the G-to-G ratios show larger dispersion around the median which is consistent with the larger inter-station distance of the pair of G stations.

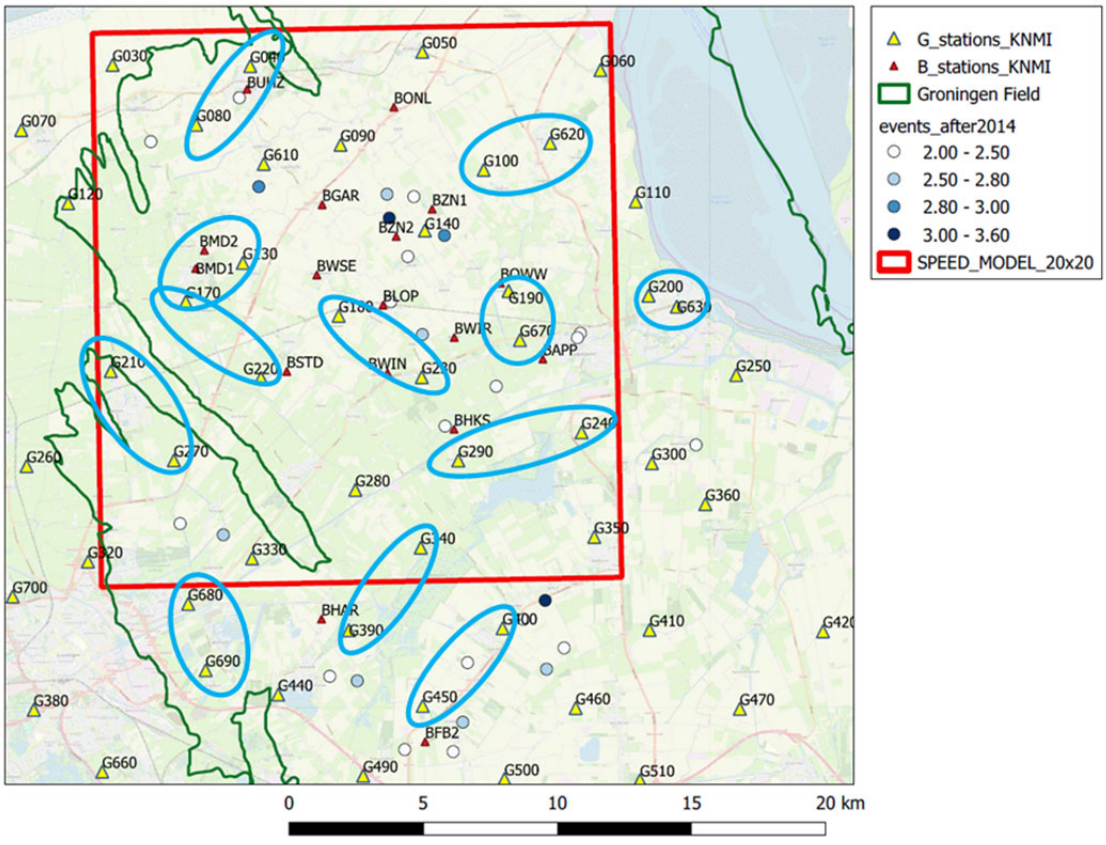

Figure 4-1 : Selected pairs of G0 stations in the Groningen field.

Table 4-1: G0 stations pairs considered in the analyses. Relative inter-station distance and number of available records are reported.

G-G pair	Inter-station distance (km)	N. of available records (FAS)	N. of available records (PSA)
G670-G190	1.87	10	7
G230-G180	3.85	10	9
G220-G170	3.97	11	6
G040-G080	2.96	5	2
G200-G630	1.13	9	7
G130-G170	2.57	9	4
G390-G340	4.08	10	9
G450-G490	3.42	11	8
G620-G110	3.84	6	2
G240-G290	4.70	4	4
G210-G270	4.06	8	3
G680-G690	2.55	3	1

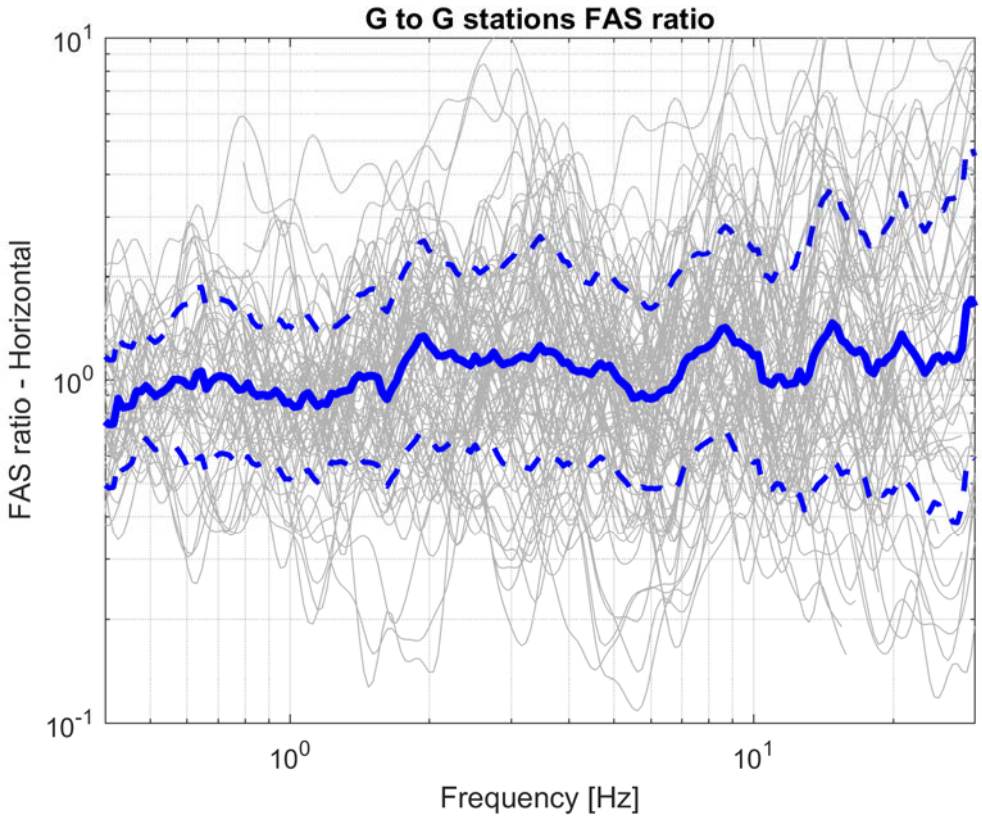

Figure 4-2 : Horizontal G-to-G Fourier Amplitude Spectra (FAS) ratio plotted for all considered pairs of stations and all events. The median ratio and its standard deviation are shown in blue.

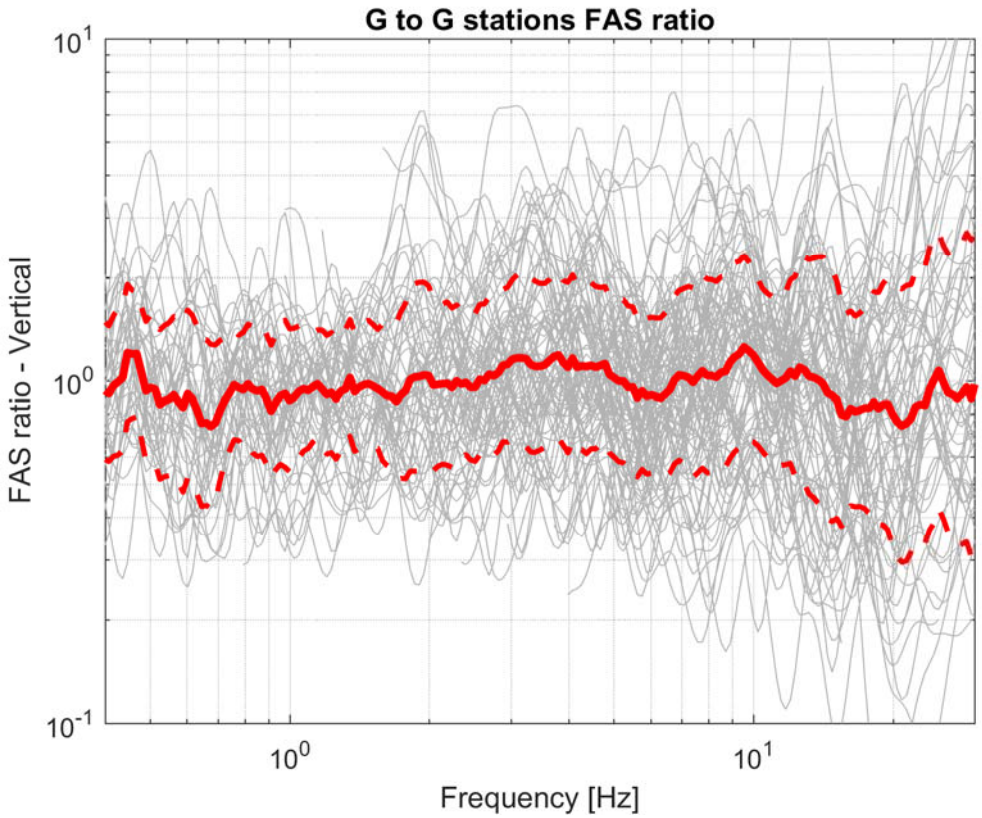

Figure 4-3 : Vertical G-to-G Fourier Amplitude Spectra (FAS) ratio plotted for all considered pairs of stations and all events. The median ratio and its standard deviation are shown in red.

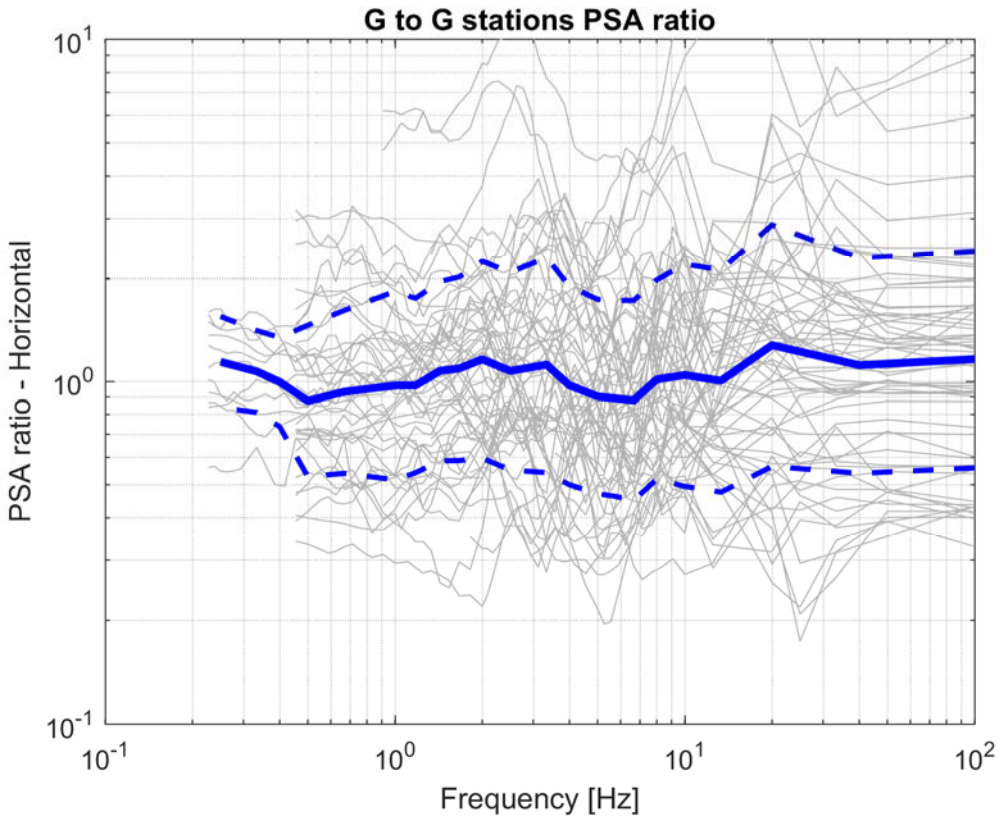

Figure 4-4 : Horizontal G-to-G spectral acceleration (PSA) ratios plotted for all considered pairs of stations and all events. The median ratio and its standard deviation are shown in blue.

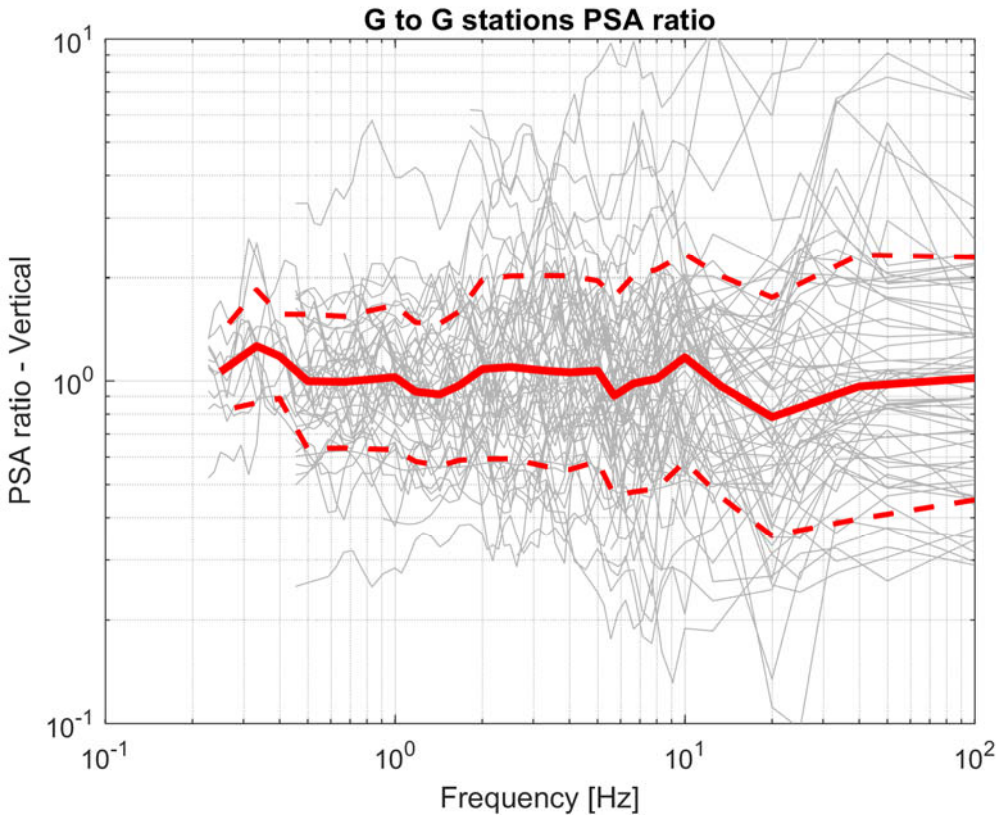

Figure 4-5 : Vertical G-to-G spectral acceleration (PSA) ratios plotted for all considered pairs of stations and all events. The median ratio and its standard deviation are shown in red.

5. Conclusions and implications for KEM04 project

Based on the results presented in this report in terms of B-to-G spectral ratios for relatively close station pairs supported by analyses of G-to-G spectral ratios (with larger interstation distance), we conclude that there are significant differences in the horizontal high-frequency ground motion recorded at most of the investigated B stations compared to that recorded at G stations. Because G stations are in most cases installed in free-field whereas B stations are installed within structures (e.g., buildings, garages), we suggest that this may be due to contamination by the structure or by artificial soil on which the sensor is installed. This is qualitatively supported by the photos of B-stations installations provided by KNMI in which the stations installed in light structures (e.g., BOWW) show on average consistent amplitudes with respect to adjacent G stations whereas stations installed within large/heavy structures (e.g., BUHZ, BMD2) depict the reduction in the high-frequencies accelerations compared to the free-field G stations.

Possible explanations that have been discussed within the KEM04 team are:

- Soil-foundation kinematic interaction that may have a filtering effect on the high-frequency ground motions, particularly on the horizontal component and in case of large structures that may require deep foundations (Stewart et al., 1999 ; Stewart, 2000).
- Velocity inversions caused by stiff artificial soils (e.g., concrete, pavement) on which the sensor is posed. As shown by Castellaro and Mulargia (2009) using noise measurements, the velocity inversion caused by such artificial soil can have a direct effect on the noise spectra and, in particular, the horizontal spectra are lowered in the high-frequency range whereas the vertical spectra are unaffected. Figure 5-1 (taken from Castellaro and Mulargia, 2009) shows an example of such effect for two simultaneous noise recordings taken respectively on natural

and artificial soil at a distance of 2 m with two instruments of identical response. The vertical component is mostly unaffected while the horizontal ones fall considerably above 5 Hz.

Further investigating the causes of the differences between B and G stations records is beyond the current scope of KEM04 project but we suggest that additional effort is needed in order to better understand and clarify the causes and the potential effects on the GMM V5.

In the KEM04 project, decision has been taken to not consider the B-station records in the continuation of the project, particularly for the calibration of the 3D numerical simulation model. B-station records will potentially be used in the comparison with the forward simulated ground motions for selected events in specific frequency bands (below 3 Hz) where a good consistency with G stations is found.

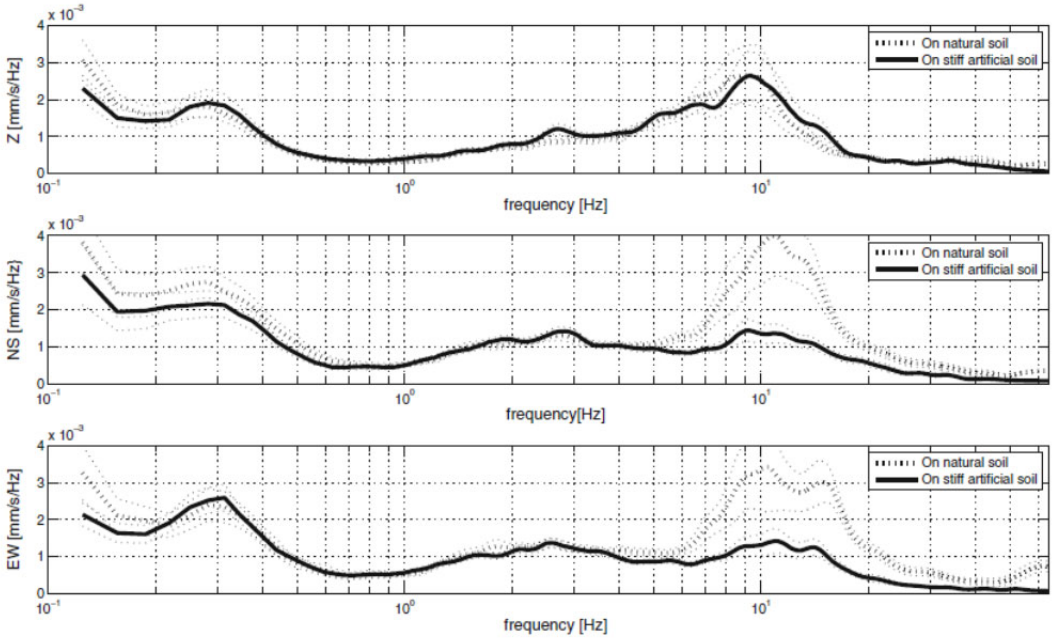

Figure 5-1 : Comparison between single spectral components recorded on natural soil vs. stiff artificial soil at the same time at two very close sites. The drop of the horizontal components is evident. (from Castellaro and Mulargia, 2009)

6. References

Akkar S, Sandikkaya MA, Senyurt M, Sisi AA, Ay BO, Traversa P, Douglas J, Cotton F, Luzi L, Hernandez B, Godey S (2014) Reference database for seismic ground-motion in Europe (RESORCE). Bull Earthq Eng 12:311–339. doi:10.1007/s10518-013-9506-8

Akkar, S., and J. J. Bommer (2006a). Influence of long-period filter cut-off on elastic spectral displacements, *Earthquake Eng. Struct. Dyn.* 35**,** no. 9, 1145–1165.

Ameri G., Oth A., Pilz M.,, Bindi D., Parolai S., Luzi L., Mucciarelli M. and G. Cultrera (2011), Separation of source and site effects by Generalized Inversion Technique using the aftershock recordings of the 2009 L'Aquila earthquake, *Bulletin of Earthquake Engineering*, 9, 717-739

Castellaro, S. and F. Mulargia (2009) The Effect of Velocity Inversions on H/V. Pure appl. geophys. 166 (2009) 567–592

Kishida T., R. E. Kayen, O-J Ktenidou, W. J. Silva, R. B. Darragh, and J. Watson-Lamprey (2014) PEER Arizona Strong-Motion Database and GMPEs Evaluation, PEER report - PEER 2014/09 Kosloff R, Kosloff D (1986) Absorbing boundaries for wave propagation problems. J Comput Phys 63(2):363–376

Konno K, Ohmachi T (1998) Ground-motion characteristics estimated from spectral ratio between horizontal and vertical components of microtremor. Bull Seismol Soc Am 88:228–241

Stewart, J.P., Seed, R. B., and G. L. Fenves (1999). Seismic soil-structure interaction in buildings. II Empirical results. *J. Geotech. Geoenviron. Eng.,* 125(1), 38–48

Stewart, J.P. (2000). "Variations between foundation-level and free-field earthquake ground motions," Earthquake Spectra, 16 (2), 511-532.

7. Annex 1: Review from KNMI scientists

A review of the draft report was performed by KNMI scientists and received from (SodM) on the 26th of April 2019. The comments and questions from KNMI (in black) as well as our replies (in red) are attached in the next pages.

Draft report: Analysis of consistency between B- and G-stations records for induced events in the Groningen gas field (STR_FUG_18P17_01)

This report investigates the consistency of data from B- and G-network data by looking at ratios of acceleration Fourier Amplitude spectra (FAS) and Pseudo Spectral Acceleration (PSA) at 5% damping.

The results show that for higher frequencies the FAS and PSA values for several B-stations are significantly smaller than recordings of adjacent G-stations. This could be due to the influence of the buildings in which the B-stations are located.

We thank the KNMI scientists for taking the time to provide comments on this study. Our replies are provided in red in the following.

General comments:

1] One of the assumptions in the study is a “relatively homogeneous local site condition” between two stations. We know that variation in P velocity is small over the network, but variation in shallow shear velocity is much higher. This is implemented in GMM development in a zonation for Groningen. Did the authors check for each station pair if the stations belong to the same zonation? The effect of the different zonation is taken into account in an amplification function, so amplitudes could be corrected for this effect.

Figure 1 below reports the zonation used in the GMM V5 and the considered B-G stations pairs. As can be seen, most of the pairs (8 out of 12) belong to the same zone whereas others belong to different zones. There is however no apparent correlation between the B-to-G spectral ratios and the fact that two stations of a pair are located or not in the same zone. For example the two pairs BOWW-G190 and BAPP-G670 are all located in zone 2111 but their mean B-to-G ratios are different (one exhibiting the high-frequency difference and the other being on average 1, See Figure 3-2 of the report). As another example, BUHZ-G040 are located in the same zone and show the difference in the high-frequency amplitudes, whereas BZN2-G140 that are located in different zones provide average ratios around 1.

As a further example, Figure 2 reports the amplification functions from the GMM V5 for zone 1032 and 1202 corresponding to the zones where BLOP and G180 are located, respectively. As can be seen the difference between the two amplification functions is minor (less than 10 % at high-frequencies).

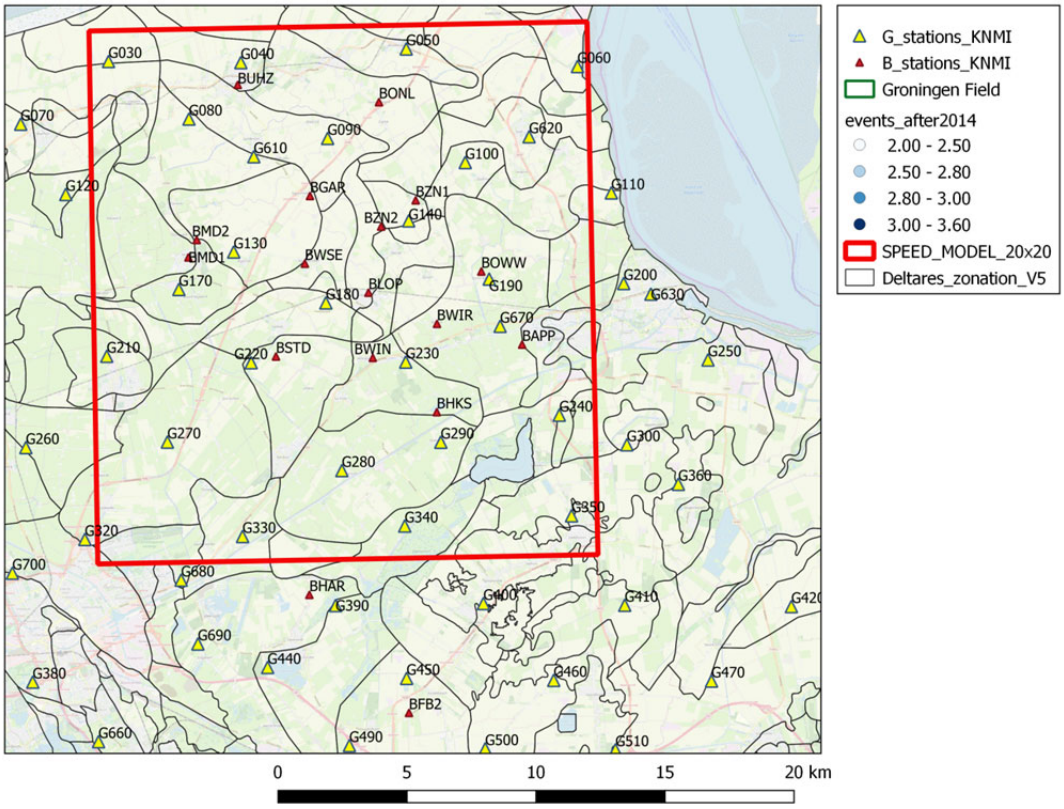

Figure 1: map of B and G stations in the Groningen field showing the GMM V5 zonation.

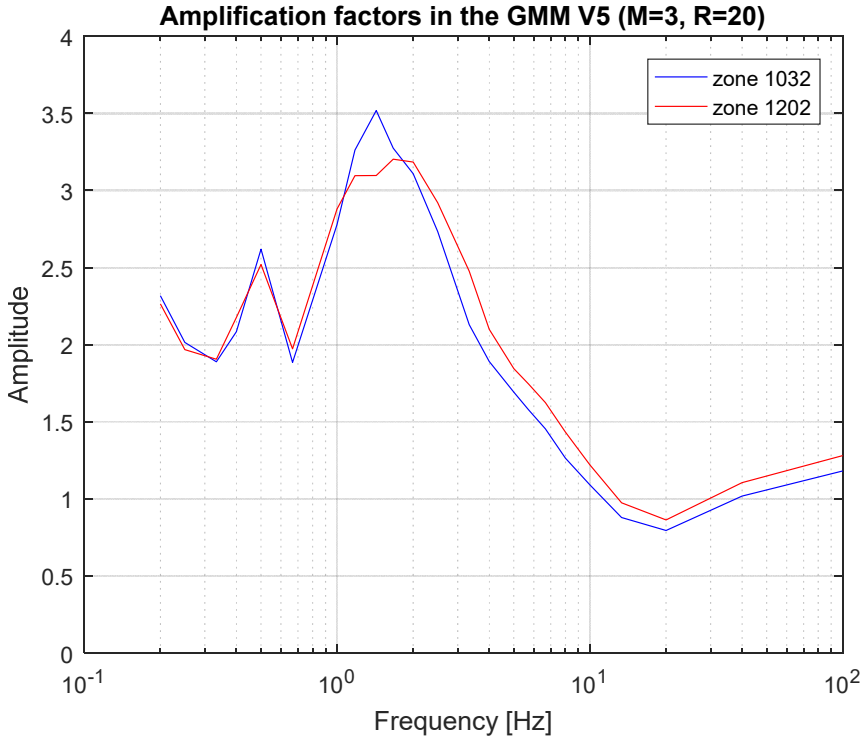

Figure 2: Amplification functions from the GMM V5 for zones where stations BLOP (1032) and G180 (1202) are located.

2] The results in Figures 3.4, 3.5, 4.2 and 4.3 show a large variability in spectral ratios as a function of frequency. There is unfortunately no discussion in the document on the significance of the results in view of the large variability in the ratio's.

These figures lump together the ratios from all the considered station pairs and, as a consequence, it is expected to see larger variability with respect to the variability of ratios for single pairs (e.g., figure 3-2). In order to show the significance of the median ratios we added in each figure the standard deviation of the distribution. We note that the standard deviation around the median for PSA ratios is of the same order of the aleatory variability of the GMM V5 and of recent GMPEs in general. For example, the σ_{ln} of the B-to-G ratios is about 0.45 for PGA which is smaller than the value of about 0.6 given by the GMM V5 (and by e.g., NGA-west 2 GMPEs). The standard deviation is slightly larger for G-to-G stations ratios (σ_{ln} =0.7) but again consistent with the GMM V5.

3] Buildings could somewhat influence the amplitudes at high frequencies, both on the horizontal and vertical components. In the report it is shown that there are no systematic differences between B and G accelerometer amplitudes on the vertical component FAS and PSA. This makes it likely that especially site conditions play a role. Obviously, people have chosen the best sites to build their villages. Moreover, sites have been improved before building, by e.g., replacement of clay by sand. Hence, on average, B-stations are likely on better sites, with less (high-frequency) amplification than in the 'free field' G-network. These shallow site conditions largely affect S-waves on the horizontal component, but do not much affect P-waves which have up till 5 times longer wavelengths in the shallow subsurface (for the same frequency) and are less affected by the reduction in shear modulus.

Our report pointed out differences between the high-frequency ground motions recorded at several adjacent B and G stations. There is no doubt that there are variations between the natural soil properties (particularly Vs) at G and B stations. The question is whether such natural variations can explain the relatively large differences observed in the amplitudes. We believe that relatively small differences in the shallow-most soil layers, as are expected between B and G stations locations, cannot explain such ground-motion differences (as also shown for example by the similar amplification functions in Figure 2 above). Of course, if much larger differences in Vs are found locally due to artificially-improved ground conditions at B stations before the building construction (as the KNMI scientists seem to suggest) this could explain the difference in the high-frequency ground motion.

Furthermore, we would like to stress that resonance effects of the building are generally well recognizable by a fundamental frequency (of the structure) that is in most cases amplified. However, it does not seem to be the case at B stations. We offer two possible alternative explanations in the report: 1. Soil-foundations kinematic interactions and 2. Decrease of the amplitude of the horizontal components due to velocity inversion caused by artificial soil on which the sensor is located. Finally assessing the origin(s) of differences in the high-frequency amplitudes of the recordings at B and G stations is beyond our scope.

Details:

P4: "KNMI communicated that an error was found in the parameterization of the G0 sensors that caused recordings of such sensors being about a factor of 2 smaller than what they should be. The G0 data have now been corrected by KNMI and they are available from their portal." → "KNMI communicated that an error was found in the parameterization of the G0 sensors that caused recordings of such sensors being a factor of 2 smaller than what they should be. The G0 data were corrected by KNMI *on December 17, 2018* and they are available from their portal."

Agreed.

P5: Td_{rup} = 2s (based on theoretical considerations, see Kishida et al., 2014): if Td_{rup} was indeed based on theoretical considerations it should be a value between a few milliseconds and about 100 ms for the considered earthquakes.

We agree. Kishida et al. (2014) suggested increasing the theoretical source duration to some extent based on empirical data. Based on Greek data with magnitude above 3.5 they proposed a source

duration of 10s which appears large for the Groningen events (mostly M =2-3). Based on preliminary tests and visual inspection of identified windows we set Td_{rup}=2s. A different Td_{rup} can be envisaged but the impact on the final results will be negligible and it will not change the conclusions of the report.

P6: what is the black vertical line in Figure 2.2 and 2.3 (last panels), please explain

The black line represents the frequency corresponding to the largest SNR.

P6: line 2: in order assess -> in order *to* assess

Corrected.

P7: Figure 2-4: the last S-wave onset pick largely affects the fitted Ts line. This pick does not make sense. It would imply that S-waves propagate relatively fast up till 30 km and afterwards slow down considerably.

The last S-wave onset pick correspond to station N030 for which windows identification seems appropriate (see figure 3), although we recognized that the S-wave onset is probably slightly later in time. As long as the main S-wave energy is included in the window, small differences in the arrival times will have a negligible impact on the selected cut-off frequencies of the filter.

We agree that the fitted polynomial Ts model is probably not appropriate for distances larger than 30-35 km and should not be extrapolated. However, it provides adequate fit to the data, especially below 30 km.

P17: “spectral rations”-> spectral ratio’s

Corrected

P18-20 Figure headers “B to G stat…”-> “G to G stat..”

Corrected

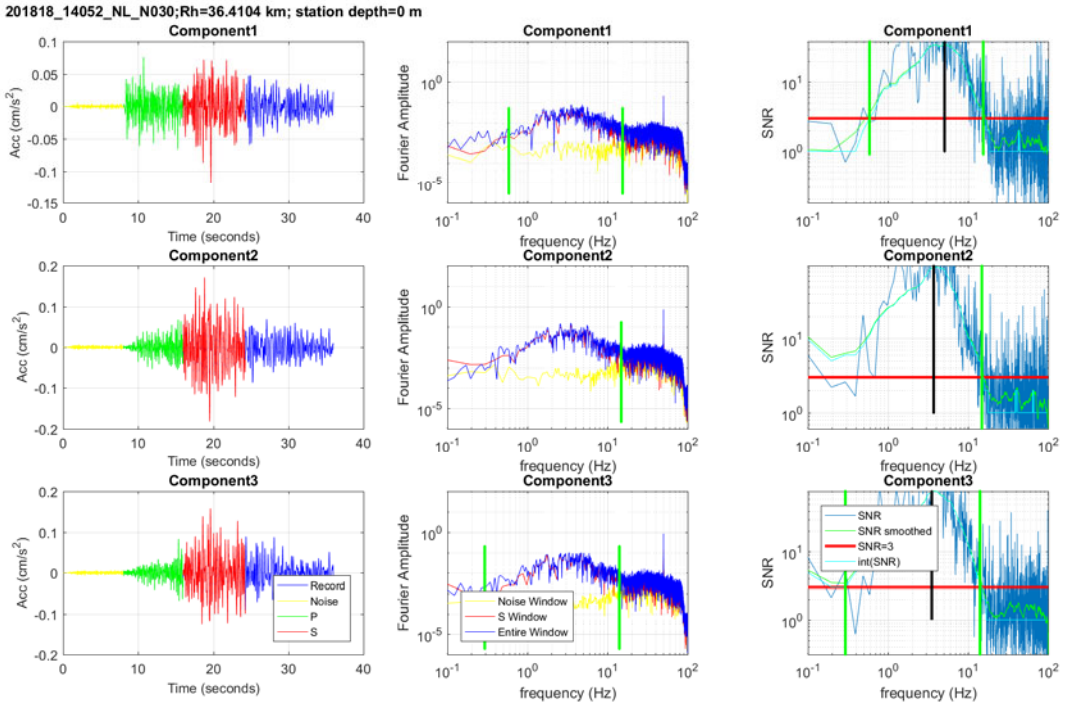

Figure 3 - Event 20180108_140052, station N030. Example of identification of P-waves, S-waves and noise windows, calculation of signal to noise (SNR) ratios and identification of high-cut and low-cut frequencies of the filter. The black line (right graphs) represents the frequency corresponding to the largest SNR.

8. Annex 2: Addendum included on 08/07/2019

This Addendum was included in the report on the 8th July 2019 upon request of SodM. It contains two additional figures of B-to-G Fourier and response spectral ratios produced in order to investigate potential dependency of the ratios as a function of the level of motion recorded.

Figure 8-1 shows the horizontal B-to-G Fourier spectral ratios. The upper-left panel is essentially the same as previously shown in Figure 3-4 except that the mean (and not the median) of the ratios from all station pairs and records is shown in blue. In the upper-right plot, the ratios are grouped according to their PGA (meaning the PGA measured at the G station of each pair). The plots in the lower panel show the ratios at two specific frequencies (F=5 Hz and F=10 Hz) as a function of PGA (lower-left) and hypocentral distance (lower-right).

Figure 8-2 shows the horizontal B-to-G response spectra (PSA) ratios. The same kind of plots made for FAS ratios are repeated here for PSA ratios with the only notable exception that in the lower panel the two selected frequencies are F=5 Hz and F=100 Hz for PSA (the latter corresponding approximately to PGA).

As a general comment we do not observe any clear trend of the FAS and PSA ratios with PGA. For the PSA ratios we observe that the mean ratio obtained for PGA larger than 10 cm/s^2 is larger than the mean ratios from smaller PGA records (Figure 8-2, upper-right plot). The mean ratio for PGA ≥ 10 cm/s^2 remains however lower than 1 for frequencies higher than about 6 Hz. This is also shown in the lower-left plot of Figure 8-2 where the PSA ratios on average increase beyond 10 cm/s^2, particularly for the 5 Hz spectral frequency. We note however that there are only few records for such PGA values and this does not allow having statistically significant conclusions of the dependency of PSA ratios on PGA.

Generally speaking, it is not clear why the observed differences between the high-frequency ground motions recorded at B and G stations should reduce with increasing PGA. In the hypothesis that such differences are due to kinematic interaction we would expect to observe rather an increase of the differences with increasing ground-motion level (see e.g., Stewart et al., 1999 ; Stewart 2000) .

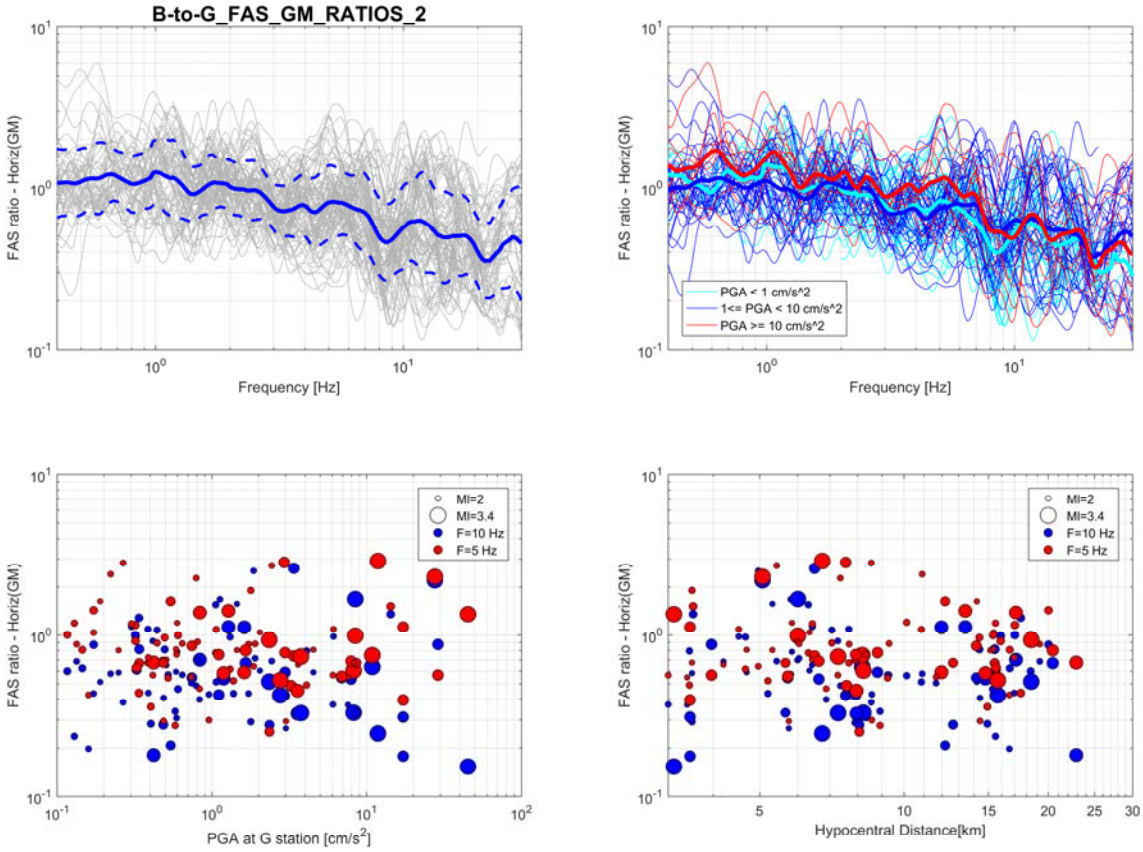

Figure 8-1 : Upper left: horizontal (geometric mean) B-to-G Fourier Amplitude Spectra (FAS) ratios plotted for all considered pairs of stations and all events. The mean ratio and its standard deviation are shown in blue. Upper right: same as in the upper left plot but color-coded according to the PGA recorded at the G station of the pair (the mean ratios for each subset are shown by thick curves). Lower left: B-to-G FAS ratios at two specific frequencies (F=5 Hz in red; F=10 Hz in blue) as a function of the PGA recorded at the G station of the pair. The size of each circle is proportional to the earthquake magnitude (MI). Lower right: same as in the lower left plot but as a function of hypocentral distance of the G stations.

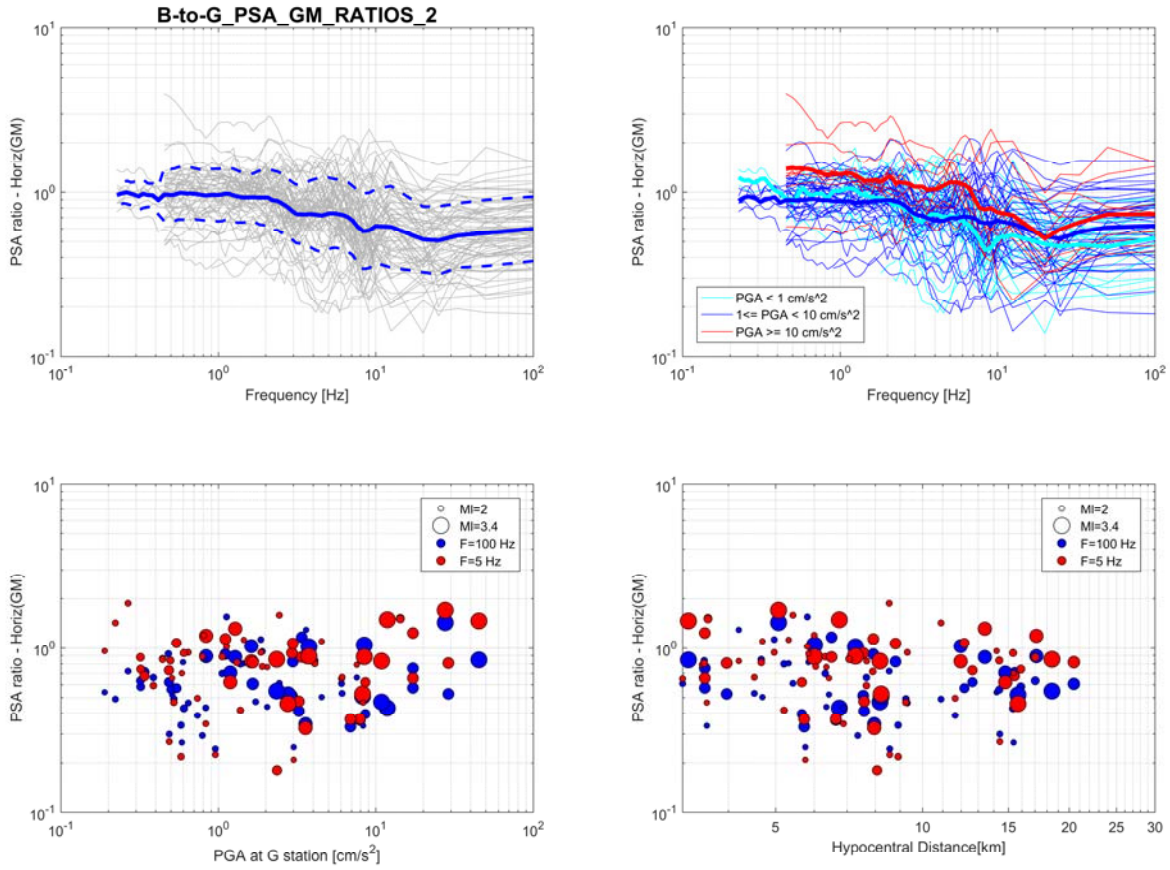

Figure 8-2 : Upper left: horizontal (geometric mean) B-to-G response spectra (PSA) ratios plotted for all considered pairs of stations and all events. The mean ratio and its standard deviation are shown in blue. Upper right: same as in the upper left plot but color-coded according to the PGA recorded at the G station of the pair (the mean ratios for each subset are shown by thick curves). Lower left: B-to-G PSA ratios at two specific frequencies (F=5 Hz in red; F=100 Hz in blue) as a function of the PGA recorded at the G station of the pair. The size of each circle is proportional to the earthquake magnitude (MI). Lower right: same as in the lower left plot but as a function of hypocentral distance of the G stations.

SEISTER
SEISMIC ENGINEERING SOLUTIONS

Seister S.A.S.
Office Montorouge
106, Avenue Marx Dormoy - 92120 Montrouge, France
Office Aubagne
Parc d'activités de Napollon
40 Avenue de Lascour - 13 400 Aubagne, France

www.seister.fr